



Embryonic and larval exposure to propylparaben induces developmental and long-term neurotoxicity in zebrafish model

Carmine Merola^{a,1}, Giulia Caioni^{b,1}, Cristiano Bertolucci^c, Tyrone Lucon-Xiccato^c, Beste Başak Savaşçı^{c,d}, Sabrina Tait^e, Marialuisa Casella^f, Serena Camerini^f, Elisabetta Benedetti^{b,*}, Monia Perugini^a

^a Department of Bioscience and Agro-Food and Environmental Technology, University of Teramo, Teramo, Italy

^b Department of Life, Health and Environmental Sciences, University of L'Aquila, L'Aquila, Italy

^c Department of Life Sciences and Biotechnology, University of Ferrara, Ferrara, Italy

^d Unit of Evolutionary Biology/Systematic Zoology, Institute for Biochemistry and Biology, University of Potsdam, Potsdam, Germany

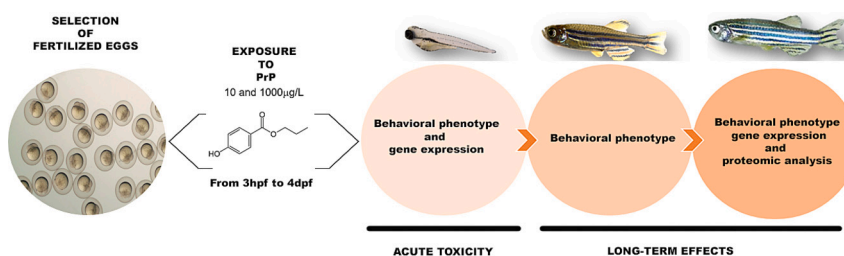
^e Gender-specific prevention and health Unit, Center for Gender-Specific Medicine, Istituto Superiore di Sanità, Rome, Italy

^f Mass Spectrometry Unit, Core Facilities, Istituto Superiore di Sanità, Rome, Italy

HIGHLIGHTS

- Propylparaben interferes with normal neurodevelopment in the zebrafish model.
- The proteomic analysis highlights Propylparaben's long-term effects on zebrafish brain development and metabolism.
- Propylparaben's effects on the brain are reflected in behavioral phenotypes at different life stages.

GRAPHICAL ABSTRACT



ARTICLE INFO

Editor: Henner Hollert

Keywords:

Parabens
Neurodevelopment
Behavior
Proteomics
Brain disorders

ABSTRACT

Parabens are preservatives found in cosmetics, processed foods, and medications. The harmful repercussions on the central nervous system by one of the most common parabens, propylparaben (PrP), are yet unknown, especially during development. In this study, the neurodevelopmental effects of PrP and long-term neurotoxicity were investigated in the zebrafish model, using an integrated approach. Zebrafish embryos were exposed to two different concentrations of PrP (10 and 1000 µg/L), then larvae were examined for their behavioral phenotypes (open-field behavior, startle response, and circadian rhythmicity) and relevant brain markers (*cyp19a1b*, *pax6a*, *shank3a*, and *gad1b*). Long-term behavioral and cognitive impacts on sociability, cerebral functional asymmetry and thigmotaxis were also examined on juveniles at 30 dpf and 60 dpf. Moreover, proteomics and gene expression analysis were assessed in brains of 60 dpf zebrafish. Interestingly, thigmotaxis was decreased by the high dose in larvae and increased by the low dose in juveniles. The expression of *shank3a* and *gad1b* genes was repressed by both PrP concentrations pointing to possible effects of PrP on neurodevelopment and

* Corresponding author at: Department of Life, Health and Environmental Sciences, University of L'Aquila, Piazzale S. Tommasi Loc., Coppito 67100, L'Aquila, Italy.

E-mail addresses: cmerola@unite.it (C. Merola), giulia.caioni@guest.univaq.it (G. Caioni), cristiano.bertolucci@unife.it (C. Bertolucci), tyrone.luconxiccato@unife.it (T. Lucon-Xiccato), basak.savasci@uni-potsdam.de (B.B. Savaşçı), sabrina.tait@iss.it (S. Tait), marialuisa.casella@iss.it (M. Casella), serena.camerini@iss.it (S. Camerini), elisabetta.benedetti@univaq.it (E. Benedetti), mperugini@unite.it (M. Perugini).

¹ These authors contributed equally.

<https://doi.org/10.1016/j.scitotenv.2023.168925>

Received 8 August 2023; Received in revised form 23 November 2023; Accepted 25 November 2023

Available online 29 November 2023

0048-9697/© 2023 The Authors. Published by Elsevier B.V. This is an open access article under the CC BY-NC-ND license (<http://creativecommons.org/licenses/by-nc-nd/4.0/>).

synaptogenesis. Proteomics analysis evidenced alterations related to brain development and lipid metabolism. Overall, the results demonstrated that early-life exposure to PrP promotes developmental and persistent neurobehavioral alterations in the zebrafish model, affecting genes and protein levels possibly associated with brain diseases.

1. Introduction

Parabens are the most prevalent ingredients in cosmetics and personal care products due to their antimicrobial, and yeast inhibitor activity (Matwiejczuk et al., 2020; Soni et al., 2001), as well as for their physicochemical properties, such as absences of color, odor and taste and good stability with other components (Janjua et al., 2007). Propylparaben (PrP) is one of the most used parabens; according to the Danish Ministry of Environment, PrP was found in 38 % of analyzed cosmetics, and personal care products with levels ranging from 0.01 to 0.32 % (Rastogi et al., 1995; Wei et al., 2021). Prp is also implied in several pharmaceutical preparations (Soni et al., 2001; Vandenberg and Bugos, 2021) and it is added to some processed foods at concentrations ranging from 200 to 450 mg/kg (Soni et al., 2001).

Due to its extensive use, PrP has contaminated several environmental matrices, including indoor dust, surface water, wastewater treatment plants, and sewage sludge (Wei et al., 2021). Based on early risk assessment conducted before 2000, parabens were considered safe for human use (Soni et al., 2005). However, later research has indicated that parabens, including PrP, may modulate or disrupt the endocrine system by binding to estrogen receptors (Nowak et al., 2018; Vandenberg and Bugos, 2021) causing impairment of female fertility, as observed in both in vivo (Vo et al., 2010). and in epidemiological studies (Smith et al., 2013). In addition, PrP levels were found 6–10 times higher in pregnant women (22.8 µg/L) than in children (0.945 µg/L) and in the general population (2.3 µg/L) (Wei et al., 2021), thus raising concerns about PrP exposure during gestation, which may affect not only mother's health but also the developing embryo/fetus. In this regard, there is limited evidence of harmful neurodevelopmental effects of PrP.

Severe pathological alterations were evidenced in brain of adult male mosquitofish treated with 240 µg/L of PrP (Ma et al., 2023) and anxiety-like behaviors associated with an increase in oxidative stress in the brain were observed in zebrafish larvae upon exposure at the embryo stage to 1 or 10 µg/L PrP (Lite et al., 2022). In support of this evidence, disruption of oxidative stress, apoptosis and fatty acid metabolism pathways was observed in zebrafish embryos treated with PrP 10 µM (Bereketoğlu and Pradhan, 2019). Alteration in lipid metabolism was also observed in a previous study by our group, in which treatment of zebrafish larvae with PrP at sublethal doses decreased neutral lipid mobilization from the yolk impairing phospholipid content in the body and the yolk sac (Perugini et al., 2019). Brain is a lipid-rich organ, so alterations of lipid content may severely affect brain functionality.

To better investigate the underlying mechanism of PrP neurodevelopmental toxicity, in the present study we adopted an integrated approach in the zebrafish model, considering different endpoints at different development stages. Zebrafish embryos were exposed for four days to PrP at 10 and 1000 µg/L, corresponding to human-relevant and sub-lethal doses (Perugini et al., 2019). Behavioral effects were observed at larvae (4 days post fertilization, dpf) and juvenile stages (30 and 60 dpf). The expression level of a panel of genes related to neurodevelopment, such as *cyp19a1b*, *pax6a*, *shank3a*, and *gad1b* (Chen et al., 2020; Cochoy et al., 2015; Forlano et al., 2001; Gonzalez-Nunez, 2015; Kikkawa et al., 2019; Kouser et al., 2013; Mei et al., 2016; Orefice et al., 2016; Peça et al., 2011; Wang et al., 2011) was assessed at both 4 and 60 dpf. Particularly, we chose *shank 3a* and *gad1b*, two genes strongly related to synaptogenesis, a sensitive target of neurotoxicity (Giordano and Costa, 2012; Rodier, 1995); *pax6a* is a master gene involved in eye development and *cyp19a1b*, also known as brain aromatase, is expressed in radial glia and involved in neuron migration and

progenitors formation. In addition, proteomic profiling of brains at 60 dpf was performed; based on the results obtained with the proteomic analysis, we also assayed *ilvbl* (alias *hacl2*) implicated in sphingolipid synthesis (Kitamura et al., 2017) and *dlg1l* (alias *dlg1b*) implicated in axon guidance and post-synaptic membrane formation (Cheung et al., 2019; Bayés et al., 2017).

2. Material and methods

2.1. Chemicals

PrP powder was purchased by Sigma-Aldrich (CAS number 94-13-3, Pharmaceutical Secondary Standard; Certified Reference Material) and dissolved in dimethyl sulfoxide (DMSO, >99.9 % purity, Sigma-Aldrich). Tricaine pharmaq (PHARMAQ AS, Norway).

2.2. Subjects' maintenance

The experiments were conducted starting from zebrafish embryos. These were obtained from AB adult wild-type zebrafish at the University of Teramo facility (protocol number n. 4236). Fish maintenance followed internationally accepted standards and was described in detail in previous studies (Merola et al., 2020a; Merola et al., 2020b). The breeding protocol consisted in selecting pairs of zebrafish (one male and one female) from the maintenance tanks and moving them overnight for habituation into separate sectors of slope breeding tanks with grid bottoms. In the following morning, the separator between two sectors of the slope tanks was removed allowing the fish to interact and spawn. The eggs were collected at 2–3 h post-fertilization (hpf). The zebrafish embryos were examined under a dissecting microscope to identify live and healthy subjects for the experiments.

2.3. Experimental treatments

The selected embryos were treated individually in 2 mL wells from 3 hpf to 4 dpf. The treatments consisted of two different concentrations of PrP, one relevant for human exposure (10 µg/L) and one inducing sublethal effects (1000 µg/L), as previously derived from Perugini et al. (2019). Prp was dissolved in DMSO, reaching the final concentration of 0.1 % of DMSO in all PrP-treated groups. Negative control, dilution water (DW) and solvent control (0.1 %DMSO) were also tested. Using a semi-static test (renewal of solution each 24 h) the concentrations of the chemical are expected to remain within ±20 % of the nominal values (as established in the OECD guidelines n.236). FET test guideline does not request quantification of zebrafish exposure solution since the small volume of each well (2 mL) make the analytical measurement unfeasible. In addition, the treatment solution was refreshed each day in each well, pre-conditioning the plates (for 24 h) with the test solutions (without embryos) before the test, to avoid adsorption of PrP to polystyrene. To control for effects of this manipulation, also control groups underwent the same solution renewal as the PrP-treated groups. Larvae hatched between 3 and 4 dpf and therefore, the subjects did not undergo solution changes outside the eggs.

2.4. Scheme of the tests performed during development

At the end of the treatments, the subjects of each treatment were split into various groups for analyses at different developmental stages. Sixty larvae per treatment group were immediately harvested at 4 dpf for gene

expression analysis (details in Section 2.8). At 5 and 6 dpf, 21–24 subjects per treatment group underwent a battery of three behavioral tests (details in Section 2.5). The remaining zebrafish were maintained following standard protocols before further testing at later developmental stages. For the maintenance, groups of subjects from the same treatment were kept in aquaria connected to a circulating system. Fish density was adjusted according to body size (20 fish per 2-l aquaria up to 30 dpf; 10 fish per 10-l aquaria thereafter). Fish were initially fed with live brine shrimps and after 15 dpf, commercial food flakes were also provided.

From the aforementioned zebrafish kept under maintenance, $N = 19$ –25 subjects per treatment was assayed at 30 dpf with two additional behavioral tests (Sections 2.5.4 and 2.5.5). Last, at 60 dpf, we performed an additional behavioral test (Section 2.5.6) to check for the persistence of long-term effects ($N = 20$ –24 per treatment). Afterwards, these zebrafish of 60 dpf were euthanized using an overdose of tricaine at 0.04 % by prolonged immersion until the cessation of opercular movement. Brain samples were dissected and analyzed by mass spectrometry ($N = 4$ per group) (details in Section 2.6), and real time-PCR ($N = 9$ per group) (details in Section 2.8).

The work was carried out following the Italian law for the protection of research animals D.L. n. 26 4 March 2014 and the European regulation directive 2010/63/U. Treatments were performed in non-feeding embryos; behavioral tests were simple observations of spontaneous swimming behavior designed to avoid distress or harms in the subjects and their protocols were approved by Ethical Committee of University of Ferrara (OPBA TLX-2022-1).

2.5. Behavioral assessment

2.5.1. Open-field test in larvae

The open-field test followed a well-established paradigm that permit assess locomotor activity and anxiety-like behavior in fish after exposure to a novel, empty environment (Ahmad and Richardson, 2013; Lucon-Xiccato et al., 2020a). It was performed on zebrafish larvae immediately after the end of PrP treatment (4 dpf). To perform the test in a novel environment, we moved the subjects into a new 24-well culture plates (TPP Tissue Culture Test Plate 24 wells, Trasadingen, Switzerland) filled with 2 mL/well of dilution water (DW). This additionally allowed us to perform the test in absence of chemicals and therefore focus on the lasting effects of our treatment. All the subjects, including the ones from the control groups, underwent this transfer with the same procedure, to ensure no confounding effects of the manipulation. The sample size for the open-field test was as follows: PrP 10 $\mu\text{g/L}$ $n = 22$; PrP 1000 $\mu\text{g/L}$ $n = 23$; solvent control $n = 24$. These subjects were assessed in three separate testing plates with 24 wells each (i.e., 3 replicates of the behavioral procedure). We took care to assign each subject to the testing plate following a pseudorandom scheme that ensured an approximately equal number of subjects from each treatment in each plate. Immediately after the transfer, the plates with the subjects were placed into a DanioVision (Noldus, Wageningen, The Netherlands) observation chamber for 60 min, isolated from external stimuli such as sound, vibration, or illumination, and fish were recorded with an IR-sensitive camera (Monochrome GigE camera, Basler, Germany). Recordings were analyzed by the EthoVision XT software (Noldus, Wageningen, The Netherlands) obtaining the following behavioral variables: activity as distance moved, activity as time spent moving, and thigmotaxis (i.e., a proxy for anxiety behavior) as time spent within one body length from the edges of the well. Data were collected in time bins of 10 min each to analyze the behavioral temporal trend.

2.5.2. Light startle response in larvae

The test consisted in exposing the larvae (4 dpf) to a sudden light stimulus and measuring their response, as previously described (Merola et al., 2021). This typically entails a marked reduction of activity and is associated with an antipredator response (Lucon-Xiccato et al., 2020b).

The startle test was conducted immediately after the open-field test, on the same sample of subjects. Therefore, the sample size and the replicates were as described in Section 2.5.1. To elicit the startle response, the light in the observation chamber was turned off for 10 min using the EthoVision software, allowing the larvae to get used to the darkness. Then the light was suddenly turned on for another 10 min to measure the reduction in the larvae's activity. The procedure was repeated three times. The activity (distance moved) in each phase of the test was recorded by the EthoVision software, to calculate a response index (proportional activity change) (Lucon-Xiccato et al., 2020b). After completion of the test, larvae were moved to new Petri dishes filled with DW, keeping individuals from different treatment groups separated, and maintained in an incubator at 28 ± 1 °C until the following day.

2.5.3. Photic entrainment of circadian behavioral rhythmicity in larvae

We then assessed the capacity of zebrafish larvae (4 dpf) circadian clock to synchronize (entrain) the behavioral activity to the daily light-dark cycle (Morbiato et al., 2019; Zarantonello et al., 2020). The photic entrainment is key to adapt to the natural alternation between day and night and due to the involvement of various systems (e.g., hormonal, sensorial, and behavioral) is often affected by stressors. To perform the test, we recorded the activity of the subjects under a light-dark alternation for 2 consecutive days.

In detail, on the day after the light startle test, the zebrafish larvae were placed one individual per well in a 96 wells culture plate (well \varnothing 0.64 cm; 96 wells per plate; Trasadingen, Switzerland), and were moved into the DanioVision chamber. Here, they were exposure to 12 h light / 12 dark photoperiods through white LED lights controlled by a computer software. The test lasted 2 days, resulting in 2 light and 2 dark phases. Accordingly, the age of larvae during this test was 5 (first day of testing) and 6 dpf (second day of testing). The software EthoVision was used to calculate distance moved by the subjects. Due to the death of two subjects between this test and the previous one, the final sample size was as follows: PrP 10 $\mu\text{g/L}$ $n = 21$; PrP 1000 $\mu\text{g/L}$ $n = 23$; solvent control $n = 23$.

2.5.4. Sociability in juveniles

The sociability of zebrafish subjects, was assessed at 30 dpf, when the ontogenetic maturation of this behavior was mostly concluded (Buske and Gerlai, 2011). In particular, we assessed fish's tendency to swim in the proximity of their mirror image (Cattelan et al., 2017), exploiting the typical misperception of their mirror image as a conspecific (Lucon-Xiccato et al., 2020c; Lucon-Xiccato and Dadda, 2017). Basically, individual zebrafish were collected from their holding tank and placed in an octagonal apparatus with mirror walls (side: 5 cm), placed on an infrared backlit table to allow tracking as described for the DanioVision observation chamber. A webcam (monochrome GigE camera, Basler, Germany) recorded the trial for 20 min, and the EthoVision software tracked the position of the subjects to calculate sociability as time spent within one body size from the mirror. In addition, the activity of each subject was calculated as distance moved. The final sample size of this test was as follows: PrP 10 $\mu\text{g/L}$ $n = 25$; PrP 1000 $\mu\text{g/L}$ $n = 19$; solvent control $n = 21$. The subjects were tested alternating the different treatment groups according to a pseudorandom scheme.

2.5.5. Cerebral functional asymmetries in juveniles

As a cognitive measure, we focused on the cerebral functional asymmetry of 30 dpf zebrafish. This can be inferred from the recordings of the sociability test because fish show eye preference to observe social stimuli, which causes them to swim in a specific direction in the apparatus (Dadda et al., 2010; Lucon-Xiccato et al., 2020c). From the recordings, we computed the time spent by subjects within one body size from the mirror swimming in a clockwise or anticlockwise direction, since these measures reflect which brain hemisphere is used by the individual to process social information. For instance, right eye preference would be due to left hemisphere processing, determining anticlockwise

swimming. A lateralization index was computed as follows: (time spent swimming clockwise – time spent swimming anticlockwise) / (time spent close to the mirror) x 100 (Lucon-Xiccato et al., 2020c). The sample size was as in the previous test (Section 2.5.4).

2.5.6. Open-field test in juveniles

211 The open-field test was repeated on 60 dpf zebrafish juveniles as described in paragraph to assess long-lasting behavioral effects. Similarly to the test performed on larvae, adult zebrafish were observed in a novel, empty environment for 20 min. The tank size was scaled to the size of the subjects (20 × 20 cm, filled with 5 cm of water) and movements tracked the movements with the same apparatus described above. The sample size was as follows: PrP 10 µg/L $n = 24$; PrP 1000 µg/L $n = 20$; solvent control $n = 22$. The subjects were tested alternating the different treatment groups.

2.6. Proteomic analysis

$N = 4$ brains per treatment group were excised from 60 dpf zebrafish and flash-frozen in nitrogen until further processing. Each brain sample was added with 100 µl Lysis Buffer (1 % NP40, 200 mM NaCl, 50 mM TRIS pH 7.4, 0.5 % Na deoxycholate), containing 1 × protease inhibitors (Sigma), and homogenized by a Micra D-1 homogenizer (ART-moderne Labortechnik, Germany), on ice for 15 min. Following centrifugation at 14,000 rpm, 4 °C for 15 min to remove debris, supernatants were collected in new tubes. Protein quantification was performed by the Pierce BCA method (Thermo Scientific, Rockford, IL, USA).

30 µg of proteins from each sample were in-solution digested after disulfide bridges reduction with 10 mM tris (2-carboxyethyl) phosphine and 16 mM iodoacetamide for the cysteins alkylation step. A solution with methanol, acetone, and ethanol (25 %, 25 %, and 50 % v/v) was added to precipitate proteins, incubating overnight at –20 °C. After centrifugation, pellets were suspended in 8 M urea and trypsin (Promega Corporation, WI, USA) in a ratio 1:50 (E:S), after the urea dilution step. After enzymatic digestion at 37 °C overnight, 20 µL of the peptide solution was injected in an Ultimate 3000 UHPLC (Dionex, Thermo Fisher Scientific, CA, USA) coupled with an Orbitrap Fusion Tribrid mass spectrometer (Thermo Fisher Scientific, CA, USA). Peptides were desalted on a trap column (Acclaim PepMap 100 C18, Thermo Fisher Scientific, CA, USA) and separated on a 20-cm-long silica capillary (Silica Tips FS 360-75-8, New Objective, MA, USA), packed in-house with a C18, 1.9 µm, 100 Å resin (Michrom BioResources, CA, USA). The analytical separation was run for 180 min using a gradient of buffer A (95 % water, 5 % acetonitrile, and 0.1 % formic acid) and buffer B (95 % acetonitrile, 5 % water, and 0.1 % formic acid) changing their percentages over time.

Full-scan MS data were acquired in the 350–1550 m/z range in the Orbitrap with 120 K resolution. Data-dependent acquisition was performed in top-speed mode (3 s long maximum total cycle): the most intense precursors were selected through a monoisotopic selection filter and with charge >1, quadrupole isolated and fragmented by higher-energy collision dissociation (32 % collision energy). Fragment ions were analyzed in the ion trap with a rapid scan rate. Raw data were analyzed by Proteome Discoverer 2.4 (Thermo Fisher Scientific, CA, USA) using the *Danio rerio* database from UniProtKB/Swiss-Prot database (Release 2022; 3228 sequences). Spectral matches were filtered using the Percolator node, based on q values, with 1 % false discovery rate (FDR). Only master proteins were considered and only specific trypsin cleavages with two miscleavages were admitted. Cysteine carbamydomethylation was set as static modification, while methionine oxidation and *N*-acetylation on the protein terminus were set as variable modifications. 15 ppm and 0.6 Da tolerance were considered for MS and MS/MS data assignment, respectively. Quantification was based on precursor intensity of unique and razor peptides using the match between runs option.

The dataset identification for all the mass spectrometry proteomics

data is MSV000091866, and it has been submitted to the ProteomeXchange Consortium through the PRIDE/MASSIVE partner repository (Perez-Riverol et al., 2019) (<https://massive.ucsd.edu/ProteomeSAFe/private-dataset.jsp?task=6f6ea2408f39459794a64f27ecbe2aba>).

2.7. Bioinformatic analysis

Raw proteomic data as protein abundances were pre-processed by the DEP 1.12.0 package (Zhang et al., 2018) in R 4.0.4 environment (R Core Team, 2021). Proteins for which more than two missing values were present in a condition were filtered out. Data were then normalized by a variance stabilizing transformation. Left-censored missing values were imputed by random draws from a Gaussian distribution centered around the first quantile of the observed values in that sample. Reduction of the batch effect was obtained using the RUVSeq 1.24.0 package setting $k = 8$ (Risso et al., 2014), then performing the differential expression analysis with edgeR 3.32.1 (McCarthy et al., 2012), controlling for the False Discovery Rate (FDR) (<5 %).

For each list of differentially expressed proteins, we performed Gene Ontology (Biological processes and Molecular functions) and KEGG enrichment analysis using the DAVID web tool (<https://david.ncifcrf.gov/>). g:Profiler (<https://biit.cs.ut.ee/gprofiler/orth> (Raudvere et al., 2019) was used to retrieve enriched Human phenotype ontologies (FDR < 10 %). The package ggplot2 3.3.6 in R was used to visualize the results.

The STRING app 1.7.1 (Doncheva et al., 2019) within Cytoscape 3.9.1 (Shannon et al., 2003) was used to retrieve protein-protein interaction networks among the proteins differentially expressed in the two treatment conditions. The g:Orth module in g:Profiler was used to transform from *Danio rerio* to *Homo sapiens* orthologous genes (encoding for the modulated proteins) then using the DisGeNET app 7.3.0 (Piñero et al., 2021) in Cytoscape to identify gene-disease network associations; the search was limited to the Disease Classes “Nervous system diseases”, “Behaviour and behavior mechanisms” and “Mental disorders”, setting the score > 0.3 and keeping associations with at least three genes.

2.8. Real-time PCR

For the gene expression analysis in the developmental life stage, $N = 60$ zebrafish larvae (4 dpf) per treatment group were anesthetized using an ice-cooling method, placed on a Petri dish positioned under a stereomicroscope and dissected to separate the head using a pair of tweezers and a needle. For each treatment groups, three groups of twenty specimens were pooled to obtain three biological replicates.

Adult zebrafish brain dissection was performed at 60 dpf and 3 pool of 9 brains for each condition ($N = 27$) were used for molecular analysis.

Samples were homogenized with a pestle and RNA extraction was performed using Trizol™ Reagent (Invitrogen, CA, USA). The NanoDrop™ 2000 Spectrophotometer (Thermo Fisher Scientific, CA, USA) was used to measure RNA purity and quantity. SuperScript IV VILOTM ezDNase Enzyme (Invitrogen, Life Technologies Corporation, CA, USA) was used for cDNA synthesis following the manufacturer's recommendations. TaqMan Universal PCR Master Mix (Thermo Fisher Scientific, CA, USA) was used to run real-time PCR reactions on an Applied Biosystem 7300 Real-Time PCR system (Applied Biosystems, CA, USA). The following gene-specific probes were used (Biorad, CA, USA): cytochrome P450, family 19, subfamily A, polypeptide 1b (*cyp19a1b*), paired box gene 6a (*pax6a*), SH3 and multiple ankyrin repeat domains 3a (*shank3a*) and glutamate decarboxylase 1b (*gad1b*), bacterial acetolactate synthase-like (*ilvbl*) and discs large MAGUK scaffold protein 1 (*dlg1*) (Table 1). The thermal cycle was as follows: 50 °C × 2 min, 95 °C × 10 min, then 40 cycles of 15-sec denaturation at 95 °C and 1 min annealing/extension at 60 °C. B-actin 1 (*actb1*) was used as the reference gene for normalizing the data. To determine the gene expression levels, we applied the $2^{-\Delta\Delta Ct}$ method (Livak and Schmittgen, 2001).

Table 1
Unique assay ID for probes purchased.

Probes	Unique assay ID
<i>cyp19a1b</i>	qDreCEP0043698
<i>pax6a</i>	qDreCEP0046155
<i>shank3a</i>	qDreCIP0047424
<i>gad1b</i>	qDreCIP0044792
<i>ilvbl</i>	qDreCIP0039168
<i>dlg1l</i>	qDreCIP0044931

2.9. Statistical analyses

Behavioral data were analyzed in R version 4.0.1 (R Core Team, 2021). Repeated measures ANOVAs were used to analyze variables implying repeated measures on each subject, fitting treatment, and the repeated measures variable (e.g., time blocks, repetition of the stimulation) as a fixed effect. This approach permitted us to study temporal variability of behavior that is particularly critical for tests performed in novel environments due to habituation. In case of significant interactions between treatment and time, we repeated the analysis testing

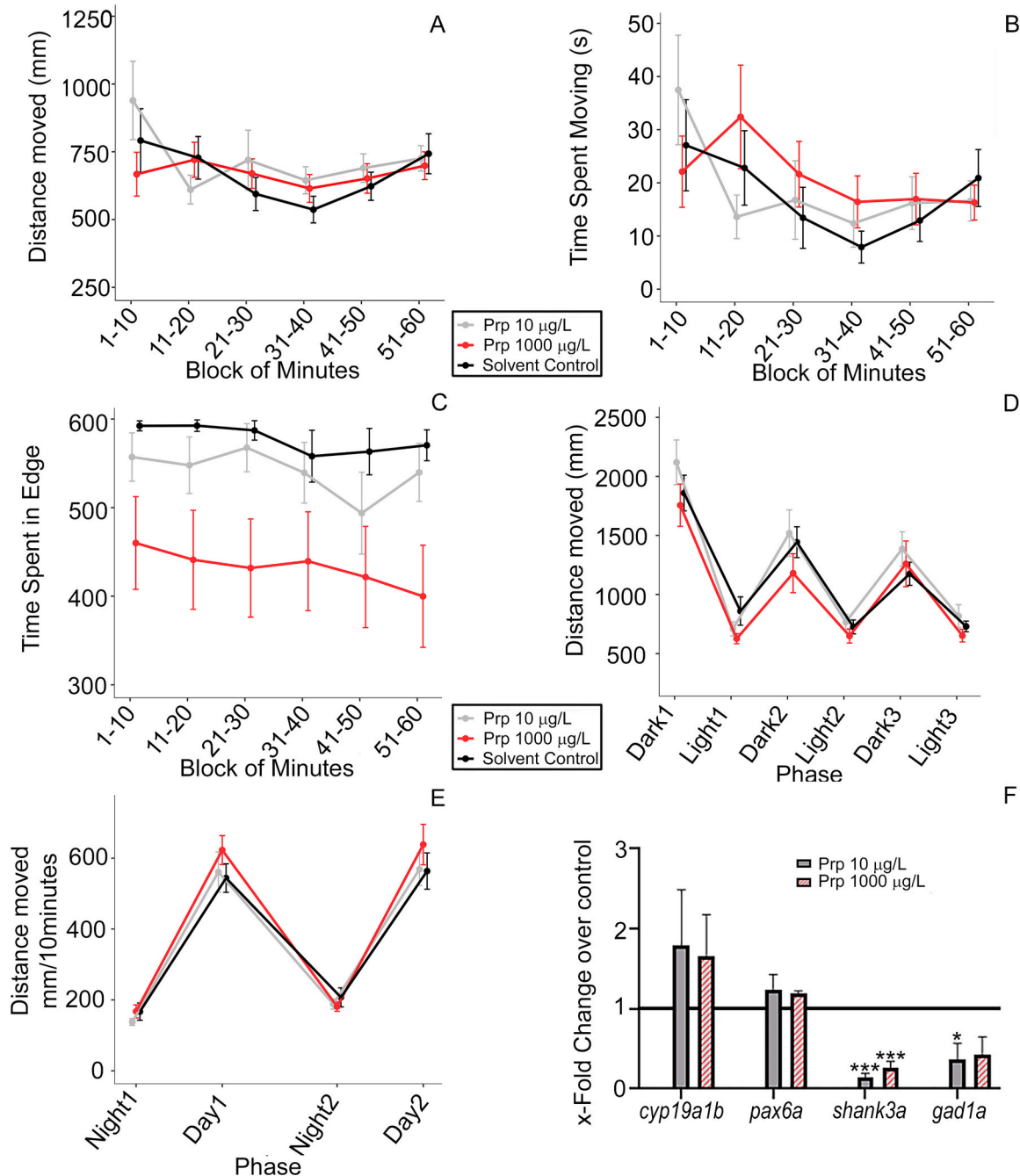


Fig. 1. Results of behavioral test and brain gene expression analysis conducted in larvae. (A) Distance moved, (B) time spent moving, and (C) time spent in the edge of the apparatus by larval subjects assayed with the open-field test (measures for each time block are shown). (D) Distance moved in the light startle test (measures for each of the six experimental phases of the assay are shown). (E) Distance moved in the photic entrainment test; data are divided into the light phase (12 h) and the dark phase of the experiment (12 h). Data represent means \pm standard errors bars. (F) Expression levels of the selected genes *cyp19a1b*, *pax6a*, *shank3a*, and *gad1b* in heads of 4 dpf larvae. 60 heads were used for each condition, in three biological replicates. Data in all the panels are means \pm SEM * indicates significant differences in transcript levels vs control (DMSO 0.1 %). * $p < 0.05$; *** $p < 0.0005$.

for an effect of treatment in each time point separately. For significant effects of the treatment, the Tukey post-hoc test was performed to compare each level. Data are expressed as estimates \pm SD.

GraphPad Prism 8 software (GraphPad Software) was used to compare statistical differences between exposed and control groups for gene expression data. Differences were deemed statistically significant for all statistical analyses if their p -values were 0.05 or lower.

3. Results

3.1. PrP effects on *4dpf* larvae

3.1.1. Behavioral experiments and gene expression assessment of relevant brain markers

3.1.1.1. Open-field test in larvae. In the open-field test, we observed no significant effect of PrP treatments on the distance moved by the larvae ($F_{2,66} = 0.355, p = 0.703$), the time block ($F_{1,342} < 0.001, p = 0.992$), or the interaction between treatment and time ($F_{2,342} = 1.303, p = 0.273$) (Fig. 1A).

A significant reduction of the time spent moving during the

observation period was observed, irrespective of the treatment ($F_{1,342} = 7.863, p = 0.005$) (Fig. 1B). However, no significant treatment \times time interaction effect was observed ($F_{2,66} = 0.495, p = 0.612$; $F_{2,342} = 0.200, p = 0.819$, respectively).

A significant treatment effect was registered for thigmotaxis ($F_{2,66} = 4.723, p = 0.012$) (Fig. 1C). In particular, Tukey's post-hoc test indicated that larvae exposed to PrP 1000 $\mu\text{g/L}$ had lower thigmotaxis compared to controls ($144.94 \pm 48.84, z = 2.968, p = 0.008$) and marginally lower thigmotaxis compared to larvae exposed to PrP 10 $\mu\text{g/L}$ ($108.56 \pm 49.92, z = 2.175, p = 0.075$). There was no difference in thigmotaxis between larvae exposed to PrP10 $\mu\text{g/L}$ and controls ($36.38 \pm 49.41, z = 0.736, p = 0.742$). Overall, the thigmotaxis significantly decreased over time ($F_{1,342} = 10.089, p = 0.002$) (Fig. 1C), but the treatment \times time interaction effect was not significant ($F_{2,342} = 0.167, p = 0.847$).

3.1.1.2. Light startle response in larvae. As expected, a significant effect of the light phase ($F_{1,330} = 386.998, p < 0.001$) was observed irrespective of the treatment, indicating a decreased activity of larvae with the light on (Fig. 1D). The effect of the repetition of the stimulus was also significant ($F_{2,330} = 16.692, p < 0.001$), indicating that larvae reduced

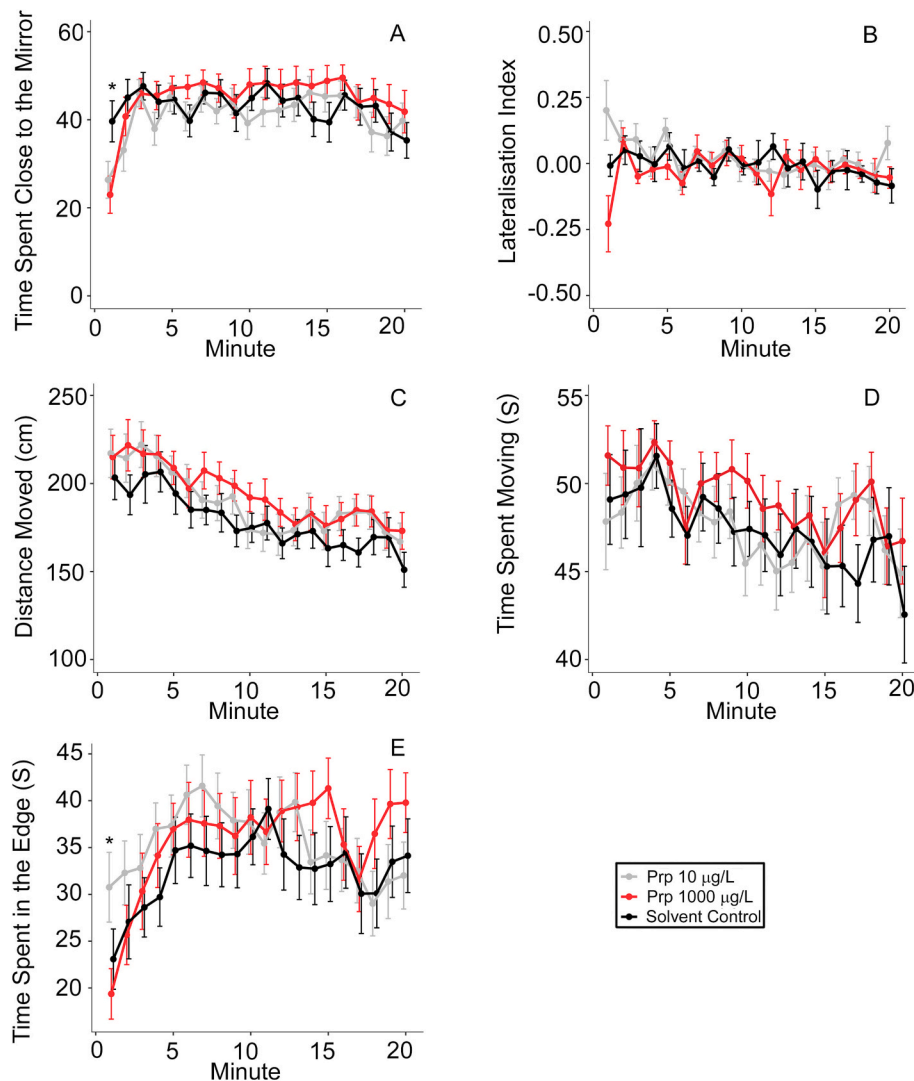


Fig. 2. Results of behavioral tests conducted in juveniles. (A) Time spent close to the mirror in the sociability test. (B) Lateralization index indicates the preference for observing the social stimulus with the right (positive values) or the left eye (negative values). (C) Distance moved, (D) time spent moving, and (E) time spent on the edge of the apparatus by juvenile subjects assayed with the open-field test. Data represent means \pm standard errors bars. * indicates significant differences in the first minute vs control (DMSO 0.1 %). $*p < 0.05$.

the activity across the three startle replicates (Fig. 1D), in particular during the dark phase (Fig. 1D), as evidenced by a significant interaction between the light phase and the replicate ($F_{2,330} = 15.632$, $p < 0.001$). The effect of treatment alone, as well as in combination with other variable effects was not significant (treatment: $F_{2,66} = 2.183$, $p = 0.121$; treatment x light phase: $F_{2,330} = 0.817$, $p = 0.443$; treatment x startle replicate: $F_{4,330} = 0.537$, $p = 0.708$; treatment x light phase x startle replicate: $F_{4,330} = 0.871$, $p = 0.481$) (Fig. 1D).

3.1.1.3. Photic entrainment of circadian behavioral rhythmicity in larvae.

Zebrafish larvae showed a significant effect of the light phase in the photic entrainment experiment ($F_{1,192} = 483.990$, $p < 0.001$) irrespective of the treatment, indicating an increased activity during the light phase compared to the dark one (Fig. 1E), in line with the typical diurnal pattern of zebrafish. However, the main effect of treatment ($F_{2,64} = 0.702$, $p = 0.499$) (Fig. 2B) as well as all the other effects and interactions were not significant ($p > 0.13$).

3.1.1.4. Gene expression assessment of relevant brain markers. The gene expression analysis in zebrafish larvae (4 dpf) evidenced a significant down-regulation of *shank3a* in zebrafish larvae treated with PrP at both concentrations ($p < 0.0005$). PrP 10 $\mu\text{g/L}$ significantly decreased *gad1b* gene expression, whereas only a downward trend was visible in the PrP 1000 $\mu\text{g/L}$ treated group (Fig. 1F).

Although not significant, an induction of *cyp19a1b* gene expression was observed in larvae exposed to PrP at both concentrations. No difference was observed for *pax6a* expression.

3.2. PrP long-term effects

3.2.1. Behavioral experiments

3.2.1.1. Sociability in juveniles. In juvenile zebrafish, we observed that although the time spent close to the mirror did not differ with treatment ($F_{2,62} = 0.716$, $p = 0.493$) and across time ($F_{1,1232} = 2.387$, $p = 0.123$); however, the interaction between treatment and time was significant ($F_{2,1232} = 6.415$, $p = 0.002$) (Fig. 2A). When we analyzed separately each time point to understand this interaction, we found that the effect of treatment was significant only in the first minute of the experiment ($F_{2,62} = 3.877$, $p = 0.026$; other p -values > 0.15), with PrP 1000 $\mu\text{g/L}$, and marginally PrP 10 $\mu\text{g/L}$, decreased zebrafish sociability compared to controls (PrP 1000 $\mu\text{g/L}$ vs. control: 16.67 ± 6.45 , $z = 2.586$, $p = 0.026$; PrP 10 $\mu\text{g/L}$ vs. control: 13.28 ± 6.03 , $z = 2.204$, $p = 0.070$) (Fig. 2A).

No significant effect was recorded on the distance moved during the sociability test in relation to treatment ($F_{2,62} = 0.382$, $p = 0.684$), time ($F_{1,1232} = 59.611$, $p < 0.001$), or their interaction ($F_{2,1232} = 1.247$, $p = 0.288$).

3.2.1.2. Cerebral functional asymmetries in juveniles. The relative lateralization index was found to significantly changed over time ($F_{1,1155} = 7.544$, $p = 0.006$) (Fig. 2B); however, no effect of treatment ($F_{2,62} = 1.505$, $p = 0.230$) or of treatment x time interaction was observed ($F_{2,1155} = 2.572$, $p = 0.077$) (Fig. 2B).

3.2.1.3. Open-field test in juveniles. The distance moved by zebrafish juveniles significantly decreased during the open-field test ($F_{1,1251} = 249.914$, $p < 0.001$), but no significant effect of treatment ($F_{2,63} = 0.949$, $p = 0.393$) or treatment x time interaction was noted ($F_{2,1251} = 0.059$, $p = 0.943$) (Fig. 2C). Similarly, also the time spent moving during the open-field test decreased with time ($F_{1,1251} = 43.843$, $p < 0.001$), but with no significant effect of treatment ($F_{2,63} = 0.465$, $p = 0.630$) or treatment x time interaction ($F_{2,1251} = 1.240$, $p = 0.290$) (Fig. 2D).

Thigmotaxis significantly increased over time ($F_{1,1251} = 8.546$, $p = 0.004$). Although the effect of treatment was not significant ($F_{2,63} = 0.459$, $p = 0.634$); a significant treatment x time interaction effect was

observed ($F_{2,1251} = 13.351$, $p < 0.001$) (Fig. 2E). Analyses separated per each minute of testing revealed that the significant interaction was due to the increased thigmotaxis in juvenile zebrafish treated with PrP 10 $\mu\text{g/L}$, during the first minute of observation. ($F_{2,63} = 3.120$, $p = 0.051$; other p -values > 0.23) (Fig. 2E).

3.2.2. Proteomics profiles of juveniles zebrafish brains

3.2.2.1. Differentially expressed proteins and functional analysis. The proteomic analysis of juveniles zebrafish brains evidenced different profiles altered by the two PrP treatments. PrP 10 $\mu\text{g/L}$ modulated a total of 142 proteins, 94 up- and 48 down-regulated, whereas PrP 1000 $\mu\text{g/L}$ modulated 186 proteins, 54 up- and 132 down-regulated. The two treatment groups shared 63 modulated proteins (Fig. 3A), mostly displaying the same up- or down-regulation, except for 17 proteins which were increased by PrP 10 $\mu\text{g/L}$ and inhibited by PrP 1000 $\mu\text{g/L}$.

By the functional enrichment analysis, we obtained only one significantly affected pathway by PrP 1000 $\mu\text{g/L}$ treatment, the *Nucleocytoplasmic transport* pathway, whereas no pathway was significantly affected by PrP 10 $\mu\text{g/L}$ (data not shown).

Several GO terms were commonly enriched by both treatment conditions (Fig. 3) but some were unique for the low and high-dose treated groups. In particular, among the most relevant GO biological processes uniquely enriched by PrP 10 $\mu\text{g/L}$ (Fig. 3B) we found the *endosome organization*, *chromatin organization*, *retrograde vesicle-mediate transport from Golgi to ER*, *mRNA processing*, *RNA splicing*, and *lipid metabolic process*. PrP 1000 $\mu\text{g/L}$ treatment exclusively enriched *heart development*, *cellular amino acid biosynthetic process*, *DNA replication*, *fatty acid metabolic process*, *cell division*, *translation*, and *neuron development* terms. The term most significantly enriched by both treatment conditions was *multicellular organism development*; further, both *protein* and *RNA transport*, as well as *brain development* were significantly affected by both PrP doses.

As regards the enriched GO metabolic function terms (Fig. 3C), the majority was affected by only one PrP concentration, except for the shared *metal ion* and *RNA binding*, as more relevant terms. PrP10 $\mu\text{g/L}$ condition was uniquely enriched in terms related to *oxidoreductase activity* and retinoid acid metabolism. On the contrary, PrP 1000 $\mu\text{g/L}$ mainly enriched terms related to enzymatic *transferase* or *lyase activity*, as well as to *nucleotide binding*.

3.2.2.2. Interaction networks. The analysis of the interactions among the proteins differentially expressed by PrP 10 $\mu\text{g/L}$ yielded three sub-networks (Fig. 4A), mostly featuring up-regulated proteins. The main hubs in the networks are represented by the repressed *gapdh* and *brd4*, and the induced *eif4ea* and *hdac3*.

A unique more complex network was identified for proteins differentially expressed by PrP 1000 $\mu\text{g/L}$ and mostly featuring repressed proteins (Fig. 4B). Also in this case *eif4ea* represented a relevant hub, although it was down-regulated by PrP 1000 $\mu\text{g/L}$, conversely to PrP 10 $\mu\text{g/L}$. Other main hubs are *rbb4l*, *pcna*, *rrm1*, *cbep1b*, *C2H6orf62*, *snrpc*, all repressed. Interestingly, the last two proteins represent “bridges” linking two sides of the network.

3.2.2.3. Gene-disease associations. By converting from *Danio rerio* to *Homo sapiens* orthologue genes (encoding the differentially expressed proteins), we explored the potential associations with Human phenotypes and Diseases.

PrP treatment enriched phenotypes all involved with abnormal brain development (Fig. 5A). In particular, the low dose PrP 10 $\mu\text{g/L}$ mostly affected brain phenotypes linked with speech and language competencies. Conversely, PrP 1000 $\mu\text{g/L}$ was mainly associated with phenotypes linked to brain abnormal morphological development.

The analysis of the possible association with brain diseases evidenced that PrP 10 $\mu\text{g/L}$ affected proteins involved in all the three

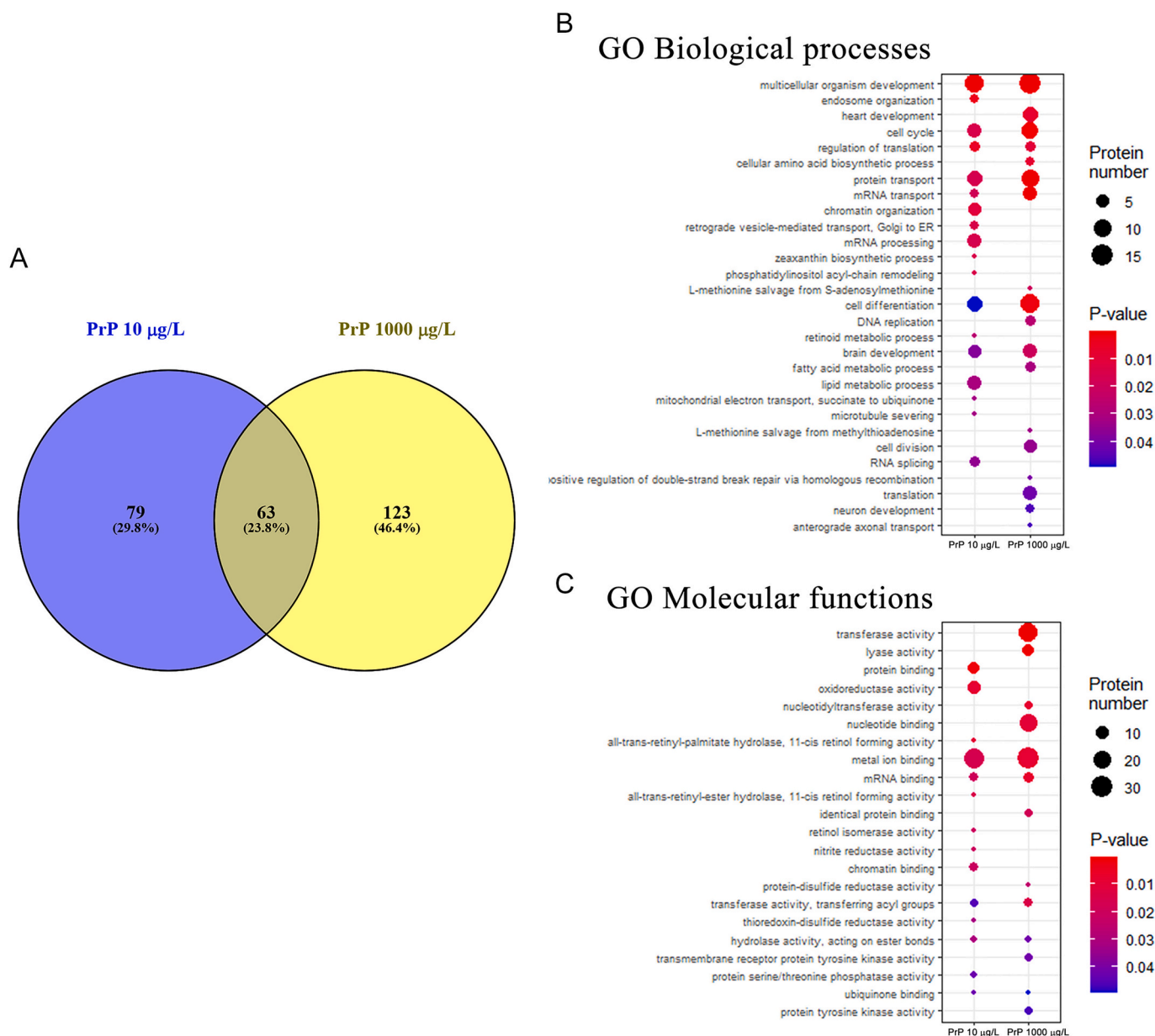


Fig. 3. (A) Venn Diagram of the protein differentially expressed in brains of juveniles zebrafish treated with PrP 10 or 1000 µg/L. (B,C) Dotplots of GO terms significantly enriched in the brains of adult zebrafish by PrP 10 µg/L and PrP 1000 µg/L treatments. The size of the points is proportional to the number of differentially expressed proteins annotated in each GO term. The color gradient from red (more significant) to blue (less significant) indicates the level of significance.

considered Disease classes, with some annotated in more classes (Fig. 5C). Most represented diseases are “Intellectual disability”, “Schizophrenia” and “Chronic alcoholic intoxication”. The more relevant hub of the network is represented by NPY, linked with several diseases. For PrP 1000 µg/L, we obtained only a limited network featuring “Intellectual Disability” associated with three genes, none overlapping with PrP10 µg/L (Fig. 5B).

3.2.3. Gene expression analysis in juveniles zebrafish

To verify long-lasting effects at the transcription level, we assessed the expression of *shank3a*, *gad1b* genes in 60 dpf zebrafish (Fig. 5D). The results confirmed the decrease of *shank3a* at least at 1000 µg/L, while no difference was observed in *gad1b* expression. Moreover, based on the results obtained with the proteomic analysis, we also assayed *ilvbl* (alias *hacl2*) and *dlg1* (alias *dlg1b*) gene expression (Fig. 5D). In agreement with the proteomic results indicating an impairment of lipid metabolism, both treatments decreased the expression level of *ilvbl*, an

enzyme of rough endoplasmic reticulum (RER) involved in alpha oxidation of phytosphingosine (Kitamura et al., 2017). The expression of *dlg1b*, a gene implicated in glutamatergic synapsis (Meyer et al., 2005), did not follow the protein trend; indeed, we observed a decrease in mRNA levels at 10 µg/L, while no change was observed at the highest concentration.

4. Discussion

PrP is a paraben extensively used in numerous daily products; as a consequence, it was detected in human matrices (Wei et al., 2021). Despite initially claimed as safe, deeper investigations have revealed potential negative effects of this class of compounds (Vo et al., 2010; Smith et al., 2013). The effects of other parabens, such as ethylparaben, butylparaben, and methylparaben, have been previously investigated in the zebrafish model supporting induction of behavioral alterations (Merola et al., 2021) and dysregulation of estrogen-regulated genes

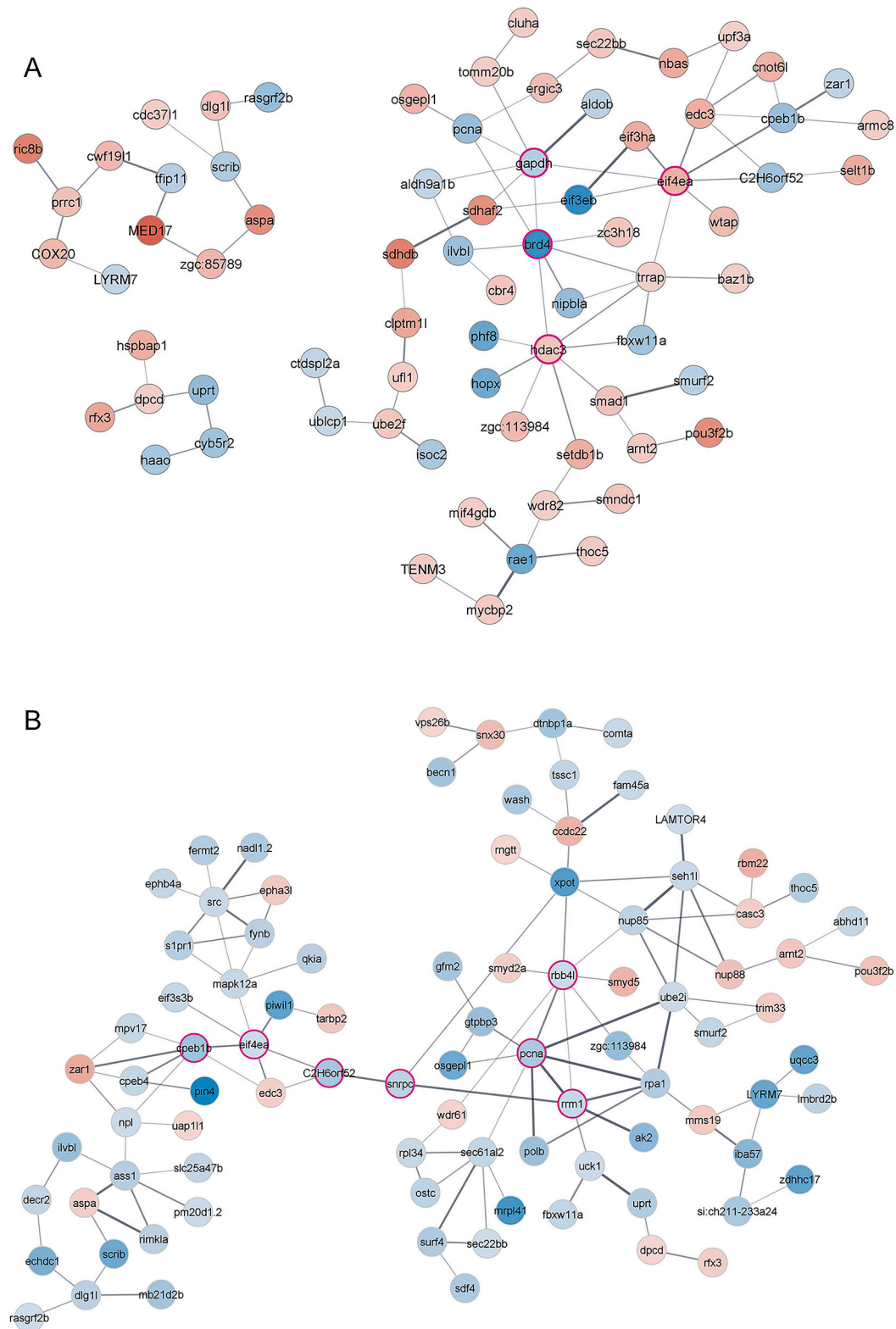


Fig. 4. Interactomes of the protein differentially expressed in juveniles zebrafish brains treated with PrP 10 µg/L (A) or PrP 1000 µg/L (B). Up-regulated and down-regulated proteins are represented with circles filled, respectively, with shades of red or blue. Magenta borders indicate the most relevant hubs in the networks.

(Bereketoglu and Pradhan, 2019; Dambal et al., 2017). So far, limited evidence is available on PrP potential neurotoxicity, especially at human-relevant concentrations. The present study highlighted that PrP early-life exposure modulates the zebrafish larval neurodevelopment by inducing persistent effects at behavioral and molecular levels until early

adulthood.

Both PrP-tested concentrations repressed *shank 3a* and *gad1b* expression, two genes strongly related to synaptogenesis, a sensitive target of neurotoxicity (Giordano and Costa, 2012; Rodier, 1995). The correct assembly of synapsis is required for the establishment of neural

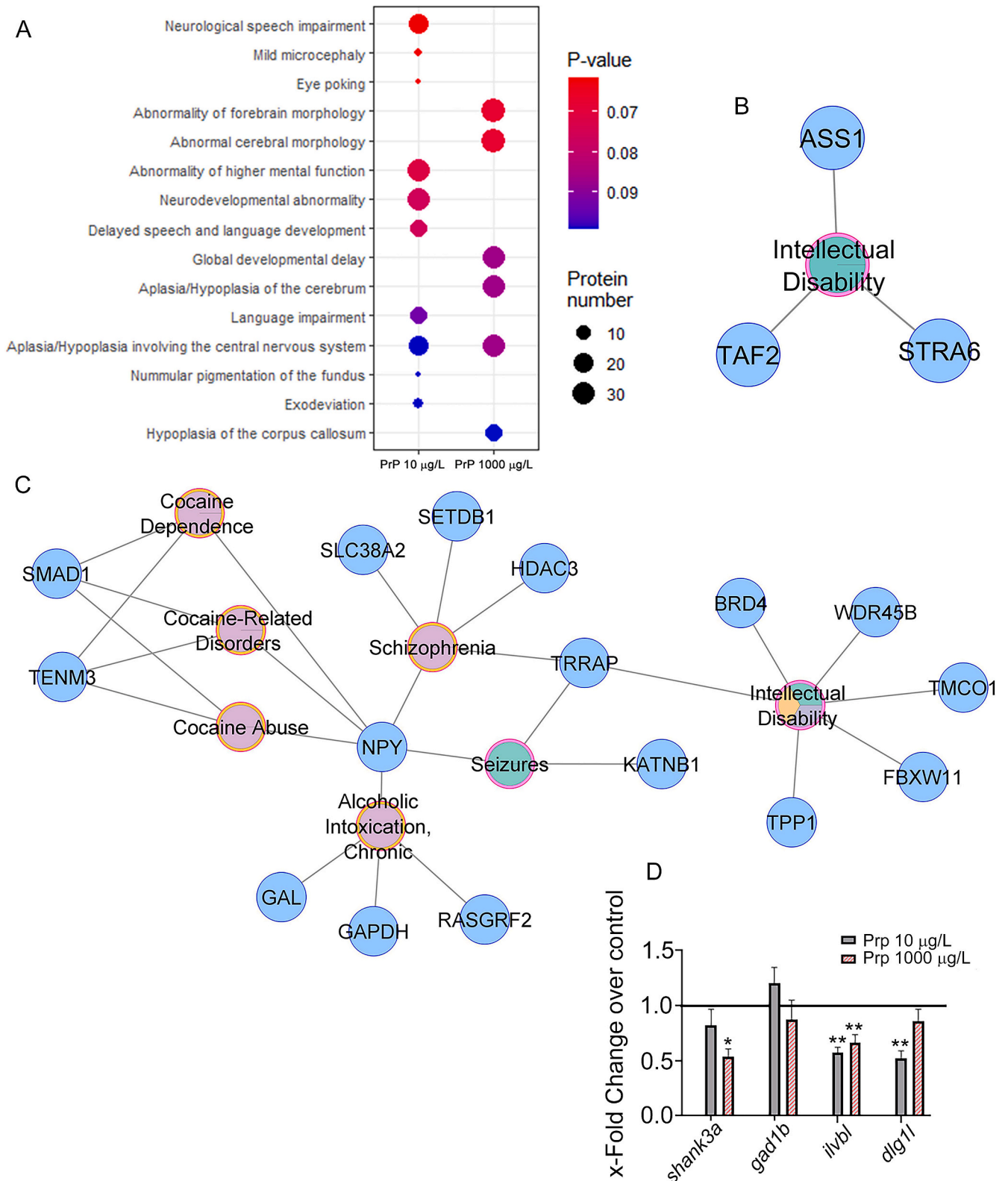


Fig. 5. (A) Human phenotypes significantly enriched in juveniles zebrafish brains by PrP 10 µg/L and PrP 1000 µg/L treatments. The size of the points is proportional to the number of featured proteins whereas significance is indicated by the red (more significant) to blue (less significant) gradient. (B, C) Gene-disease association networks in juveniles zebrafish brains induced by PrP 10 µg/L (C) and PrP 1000 µg/L (B) treatments. Disease colors indicate the category: pink for “Mental disorders”, green for “Nervous System Diseases”, and orange for “Behavior and Behavior Mechanisms”. (C) Gene Expression levels of the selected genes shank3a, gad1b, ilvbl, dlg1l in 60 dpf specimens. Shank3a, gad1b, ilvbl, dlg1l were assessed in 9 brains for each condition of 60 dpf zebrafish. Data are presented as means ± SEM. * indicates significant differences in transcript levels vs control (DMSO 0.1 %). **p* < 0.05; ***p* < 0.005.

networks, and consequently for the development of normal cognitive abilities and behavior, while altered synapse assembly may lead to neurological disorders (Washbourne, 2015). *Shank 3a* belongs to the Shank/ProSAP family of proteins, including scaffolding proteins crucial for synaptic development and function, (Sheng and Kim, 2000) and for spine morphogenesis and synaptic plasticity (Sarowar and Grabrucker, 2016). PrP exposure repressed the expression of *shank3a* in both zebrafish larvae and juveniles. The ortholog of human SHANK3 is duplicated in the zebrafish genome as *shank3a* and *shank3b* during teleost evolution (Kaluff et al., 2014). Loss-of-function mutations in zebrafish, to generate *shank3b*^{-/-} and *shank3ab*^{-/-} models, induced pervasive developmental delay, impaired social preference, repetitive swimming behaviors, and generally reduced locomotor activity (Liu et al., 2018, 2021). Adult zebrafish *shank3b*^{-/-} showed reduced thigmotaxis, duration, and frequency of social contacts with the peer group, decreased time ratio and distance ratio in the conspecific sector, and reduced kin recognition and preference (Liu et al., 2018). Although this pattern did not completely overlap with our behavioral data, especially those in juveniles (see discussion below), it would be interesting to functionally associate *shank3a* with PrP-mediated behavioral alterations.

The *gad1b* gene encodes for the rate-limiting enzyme catalyzing the synthesis of γ -amino butyric acid (GABA) through the oxidative decarboxylation of glutamate. GABA exerts inhibitory function in the adult brain, shifting from excitation by a progressive decrease in intracellular chloride ion concentration (Zhang et al., 2010). GABA is also involved in neuronal migration, neuronal arbor elaboration, differentiation, and synapse formation during neurodevelopment (Kriegstein and Owens, 2001; Represa and Ben-Ari, 2005). The observed reduction of *gad1b* gene expression level in larvae is in line with the decrease in *shank3a* mRNA content, suggesting an impact of PrP on excitatory synapse formation. Moreover, *pax6a* and *cyp19a1b* expression in larvae did not change, suggesting that the major effects of PrP on CNS is on correct assembly of synapsis rather than neural progenitors formation. In juveniles, the mRNA expression level seems to be restored at both treatment conditions, according to the shift from excitation to inhibitory function of GABA in adult teleosts.

The behavioral experiments provided support, albeit limited, to the alterations highlighted by the gene expression data. We observed that thigmotaxis was significantly affected by PrP treatment, but with diverging effects in larval and juvenile individuals, in agreement with *shank3a* and *gad1b* mRNA expression. Indeed, zebrafish larvae exposed to PrP 1000 $\mu\text{g/L}$ showed reduced thigmotaxis in the open-field test whereas zebrafish juveniles exposed to PrP 10 $\mu\text{g/L}$ displayed evidence of increased thigmotaxis. Thigmotaxis is a validated index of anxiety, which is evolutionarily conserved in teleost fish, including zebrafish (Schnörr et al., 2012). High anxiety levels are expected to increase thigmotaxis behavior (Lucon-Xiccato et al., 2020a) because the animal searches for enclosed spaces as a defensive response (Higaki et al., 2018). Thus, exposure to PrP at the higher dose reduced anxiety-like behavior soon after exposure, but the lower dose had a long-lasting effect on increasing anxiety in juveniles, possibly determined by the early repression of *gad1b*. It is worth noting that the effect showed by larvae was extremely marked and evident throughout the entire test, while the effect in the juveniles was limited to the first minute of testing. The open-field test is based on the behavior of the animals as soon as it is exposed to a novel environment. Therefore, the response is expected to be high at the beginning of the test and then progressively reduce due to habituation to the novel environment. We speculate that the transient effect observed in juvenile subjects may be due to this phenomenon, as well as possibly to a smaller effect size compared to that showed by larvae. Accordingly, a previous study on a fish model found that the decrease in the response to the open-field test was not clearly defined in subjects with age of 30 or less days, and because evident during later developmental stages (Lucon-Xiccato et al., 2020a). Interestingly, PrP effects on anxiety diverged from those of previously studied parabens in

the zebrafish model (Merola et al., 2021), possibly due to different chemical properties, and different toxicological profiles (Merola et al., 2020a; Merola et al., 2020b; Perugini et al., 2019). Considering the remaining behavioral analyses, we found limited evidence of effects due to PrP. With the exception of thigmotaxis, the behavioral variables collected in the open-field test did not differ between the experimental groups. Furthermore, PrP exposure did not impair the visual startle response and the circadian photic entrainment in zebrafish larvae as similarly observed for other parabens (Merola et al., 2021). Indeed, the gene expression of *pax6*, a master regulator of eye development, both in vertebrates and invertebrates (Klann and Seaver, 2019; Nishina et al., 1999) was not affected by both PrP doses. Last, we found that juvenile subjects exposed to both PrP concentrations also exhibited evidence of lower sociability, but this effect was transient and visible only at the beginning of the test. Thus, early PrP exposure may have later effects also on this behavioral endpoint, although our data are not conclusive. In adults, the mRNA expression level seems to be restored at both treatment conditions, according to the shift from excitation to inhibitory function of GABA in adult teleosts, and this may explain the small effect detected on sociability. Certainly, further ethological analyses associated with molecular and biochemistry indicators should be performed to support the behavioral findings of this study.

The proteomic analysis performed at 60 dpf evidenced further long-term effects induced by the two PrP dose treatments, which significantly affected GO terms related to brain development, but also to lipid metabolism, highly relevant for synapsis. As a confirmation, the gene expression of *ilvbl*, an enzyme of the RER involved in the alpha oxidation of phytosphingosine, and thus in sphingolipid synthesis (Kitamura et al., 2017), was repressed by both treatment doses. Thus PrP, by altering the lipid metabolism, may have further determined a synaptic dysfunction due to defective dynamics of synaptic membranes, with a compromised formation of synaptic vesicles and their release.

Importantly, among the 63 proteins commonly modulated by the two PrP doses, 17 were induced by PrP 10 $\mu\text{g/L}$ and repressed by PrP 1000 $\mu\text{g/L}$ and featuring relevant regulators of neurodevelopmental processes. Among them, *tenm3* is involved in dendrite guidance and visual perception, while *dlg1l* regulates post-synaptic membrane formation; both are involved in axon guidance (Cheung et al., 2019; Bayés et al., 2017). Although we observed a decreased gene expression of *dlg1l* in adult zebrafish exposed to PrP 10 $\mu\text{g/L}$, the lack of consistency with protein expression may be due to unknown underlying regulatory mechanisms. However, it confirms that *dlg1l* is a sensitive endpoint.

Moreover, the interaction networks confirmed a major involvement of induced proteins in the PrP 10 $\mu\text{g/L}$ group and of repressed proteins in the PrP 1000 $\mu\text{g/L}$ one. Some of the identified hubs in the interactomes were associated with neurological diseases, especially in PrP 10 $\mu\text{g/L}$ treated zebrafish, such as *hdac3*, associated with schizophrenia and *brd4* with intellectual disability. *Hdac3* association may be ascribed to its function as a deacetylase enzyme (Večeřa et al., 2018), while *brd4*, an epigenetic regulator, may play a role in the DNA repair pathway, as evidenced in the Cornelia de Lange syndrome, characterized by intellectual disability (Olley et al., 2021). Both factors interact with *trapp*, a histone acetyltransferase cofactor regulating mitotic checkpoint and cell cycle (Herceg et al., 2001), and associated with schizophrenia and intellectual disability (Huang et al., 2022; Xu et al., 2012). These associations are also supported by the analysis of human phenotypes in which speech and language as well as higher mental functions may be impaired by PrP 10 $\mu\text{g/L}$ treatment. The PrP 1000 $\mu\text{g/L}$ treated group was found associated only with intellectual disability and most significant human phenotypes were related to abnormal brain morphology, supported by the interactome mostly featuring repressed proteins.

These findings molecularly confirm previous phenotypical evidence in zebrafish larvae exposed to PrP 1000 and 10 $\mu\text{g/L}$ for 96 hpf, displaying a reduction of embryo length and head size, with evident craniofacial malformations and decreased lipids in the body (Perugini et al., 2019). Since PrP 10 $\mu\text{g/L}$ is a human-relevant concentration, a

refinement of its use in commercial products could be advantageous.

5. Conclusions

The results of the present study revealed for the first time that early-life exposure to PrP induced developmental and persistent neuro-behavioral changes in the zebrafish model. Thigmotaxis was affected in both zebrafish larvae and juveniles, albeit less markedly, and additionally reduced sociability was observed only in zebrafish juveniles. At a molecular level, the highest dose displayed a strong repressing effect on relevant brain developmental processes otherwise, the lowest dose modulated relevant signaling and proteins possibly associated with mental and behavioral disorders later in life. This raises concern about human exposure to PrP since the 10 µg/L dose is human-relevant, thus a refined risk assessment of this compound is advisable to protect the most vulnerable population and avoid later effects such as neurodegenerative disorders in adulthood. Further, *in vivo* studies are required to better clarify the mechanistic pathways of PrP neurotoxicity and to elucidate the contribution of environmental PrP exposure to human neurodevelopmental disorders.

Funding

This work received financial support from FFO BenedettiUnivaq.

CRediT authorship contribution statement

Carmine Merola: Data curation, Formal analysis, Investigation, Methodology, Writing – review & editing. **Giulia Caioni:** Data curation, Formal analysis, Investigation, Methodology, Writing – review & editing. **Cristiano Bertolucci:** Formal analysis, Methodology, Writing – review & editing, Supervision. **Tyrone Lucon-Xiccato:** Formal analysis, Methodology, Writing – review & editing. **Beste Başak Savaşçı:** Formal analysis, Methodology, Writing – review & editing. **Sabrina Tait:** Formal analysis, Methodology, Writing – review & editing, Supervision. **Marialuisa Casella:** Formal analysis, Methodology, Writing – review & editing. **Serena Camerini:** Formal analysis, Methodology, Writing – review & editing. **Elisabetta Benedetti:** Conceptualization, Data curation, Funding acquisition, Project administration, Supervision, Writing – original draft. **Monia Perugini:** Conceptualization, Data curation, Project administration, Supervision, Writing – original draft.

Declaration of competing interest

The authors affirm that they have no known financial or interpersonal conflicts that would have appeared to have an impact on the research presented in this study.

Data availability

Data will be made available on request.

Acknowledgments

The authors wish to thank Andrea Margutti for building the apparatuses of behavioral tests.

References

- Ahmad, F., Richardson, M.K., 2013. Exploratory behaviour in the open field test adapted for larval zebrafish: impact of environmental complexity. *Behav. Processes* 92, 88–98. <https://doi.org/10.1016/j.beproc.2012.10.014>.
- Bayés, A., Collins, M.O., Reig-Viader, R., Gou, G., Goulding, D., Izquierdo, A., Choudhary, J.S., Emes, R.D., Grant, S.G.N., 2017. Evolution of complexity in the zebrafish synapse proteome. *Nat. Commun.* 8, 14613. <https://doi.org/10.1038/ncomms14613>.

- Bereketoğlu, C., Pradhan, A., 2019. Comparative transcriptional analysis of methylparaben and propylparaben in zebrafish. *Sci. Total Environ.* 671, 129–139. <https://doi.org/10.1016/j.scitotenv.2019.03.358>.
- Busse, C., Gerlai, R., 2011. Shoaling develops with age in zebrafish (*Danio rerio*). *Prog. Neuropsychopharmacol. Biol. Psychiatry* 35, 1409–1415. <https://doi.org/10.1016/j.pnpb.2010.09.003>.
- Cattelan, S., Lucon-Xiccato, T., Pilastro, A., Griggio, M., 2017. Is the mirror test a valid measure of fish sociability? *Anim. Behav.* 127, 109–116. <https://doi.org/10.1016/j.anbehav.2017.03.009>.
- Chen, Q., Deister, C.A., Gao, X., Guo, B., Lynn-Jones, T., Chen, N., Wells, M.F., Liu, R., Goard, M.J., Dimidschstein, J., Feng, S., Shi, Y., Liao, W., Lu, Z., Fishell, G., Moore, C.I., Feng, G., 2020. Dysfunction of cortical GABAergic neurons leads to sensory hyper-reactivity in a Shank3 mouse model of ASD. *Nat. Neurosci.* 23, 520–532. <https://doi.org/10.1038/s41593-020-0598-6>.
- Cheung, A., Trevers, K.E., Reyes-Corral, M., Antinucci, P., Hindges, R., 2019. Expression and roles of teneurins in zebrafish. *Front. Neurosci.* 13, 158. <https://doi.org/10.3389/fnins.2019.00158>.
- Cochoy, D.M., Kolevzon, A., Kajiwar, Y., Schoen, M., Pascual-Lucas, M., Lurie, S., Buxbaum, J.D., Boeckers, T.M., Schmeisser, M.J., 2015. Phenotypic and functional analysis of SHANK3 stop mutations identified in individuals with ASD and/or ID. *Mol. Autism* 6, 23. <https://doi.org/10.1186/s13229-015-0020-5>.
- Dadda, M., Domenichini, A., Piffer, L., Argenton, F., Bisazza, A., 2010. Early differences in epithalamic left–right asymmetry influence lateralization and personality of adult zebrafish. *Behav. Brain Res.* 206, 208–215. <https://doi.org/10.1016/j.bbr.2009.09.019>.
- Dambal, V.Y., Selvan, K.P., Lite, C., Barathi, S., Santosh, W., 2017. Developmental toxicity and induction of vitellogenin in embryo-larval stages of zebrafish (*Danio rerio*) exposed to methyl Paraben. *Ecotoxicol. Environ. Saf.* 141, 113–118. <https://doi.org/10.1016/j.ecoenv.2017.02.048>.
- Doncheva, N.T., Morris, J.H., Gorodkin, J., Jensen, L.J., 2019. Cytoscape StringApp: network analysis and visualization of proteomics data. *J. Proteome Res.* 18, 623–632. <https://doi.org/10.1021/acs.jproteome.8b00702>.
- Forlano, P.M., Deitcher, D.L., Myers, D.A., Bass, A.H., 2001. Anatomical distribution and cellular basis for high levels of aromatase activity in the brain of teleost fish: aromatase enzyme and mRNA expression identify glia as source. *J. Neurosci.* 21, 8943–8955. <https://doi.org/10.1523/JNEUROSCI.21-22-08943.2001>.
- Giordano, G., Costa, L.G., 2012. Developmental Neurotoxicity: Some Old and New Issues. *International Scholarly Research Notices* 2012, e814795. <https://doi.org/10.5402/2012/814795>.
- Gonzalez-Nunez, V., 2015. Role of gabra2, GABAA receptor alpha-2 subunit, in CNS development. *Biochem. Biophys. Rep.* 3, 190–201. <https://doi.org/10.1016/j.bbrep.2015.08.003>.
- Herceg, Z., Huila, W., Gell, D., Cuenin, C., Leonart, M., Jackson, S., Wang, Z.Q., 2001. Disruption of Trpapp causes early embryonic lethality and defects in cell cycle progression. *Nat. Genet.* 29, 206–211. <https://doi.org/10.1038/ng725>.
- Higaki, A., Mogi, M., Iwanami, J., Min, L.-J., Bai, H.-Y., Shan, B.-S., Kan-no, H., Ikeda, S., Higaki, J., Horiuchi, M., 2018. Recognition of early stage thigmotaxis in Morris water maze test with convolutional neural network. *PLoS One* 13, e0197003. <https://doi.org/10.1371/journal.pone.0197003>.
- Huang, Y.-S., Fang, T.-H., Kung, B., Chen, C.-H., 2022. Two genetic mechanisms in two siblings with intellectual disability, autism spectrum disorder, and psychosis. *J. Pers. Med.* 12, 1013. <https://doi.org/10.3390/jpm12061013>.
- Janjua, N.R., Mortensen, G.K., Andersson, A.-M., Kongshoj, B., Skakkebaek, N.E., Wulf, H.C., 2007. Systemic uptake of diethyl phthalate, dibutyl phthalate, and butyl paraben following whole-body topical application and reproductive and thyroid hormone levels in humans. *Environ. Sci. Technol.* 41, 5564–5570. <https://doi.org/10.1021/es0628755>.
- Kaluuff, A.V., Stewart, A.M., Gerlai, R., 2014. Zebrafish as an emerging model for studying complex brain disorders. *Trends Pharmacol. Sci.* 35, 63–75. <https://doi.org/10.1016/j.tips.2013.12.002>.
- Kikkawa, T., Casingal, C.R., Chun, S.H., Shinohara, H., Hiraoka, K., Osumi, N., 2019. The role of Pax6 in brain development and its impact on pathogenesis of autism spectrum disorder. *Brain Res.* 1705, 95–103. <https://doi.org/10.1016/j.brainres.2018.02.041>.
- Kitamura, T., Seki, N., Kihara, A., 2017. Phytosphingosine degradation pathway includes fatty acid α -oxidation reactions in the endoplasmic reticulum. *Proc. Natl. Acad. Sci.* 114, E2616–E2623. <https://doi.org/10.1073/pnas.1700138114>.
- Klann, M., Seaver, E.C., 2019. Functional role of pax6 during eye and nervous system development in the annelid *Capitella teleta*. *Dev. Biol.* 456, 86–103. <https://doi.org/10.1016/j.ydbio.2019.08.011>.
- Kouser, M., Speed, H.E., Dewey, C.M., Reimers, J.M., Widman, A.J., Gupta, N., Liu, S., Jaramillo, T.C., Bangash, M., Xiao, B., Worley, P.F., Powell, C.M., 2013. Loss of predominant Shank3 isoforms results in hippocampus-dependent impairments in behavior and synaptic transmission. *J. Neurosci.* 33, 18448–18468. <https://doi.org/10.1523/JNEUROSCI.3017-13.2013>.
- Kriegstein, A.R., Owens, D.F., 2001. GABA May Act as a Self-limiting Trophic Factor at Developing Synapses. *Sci STKE* 2001, pe1. <https://doi.org/10.1126/stke.2001.95.pe1>.
- Lite, C., Guru, A., Juliet, M., Arockiaraj, J., 2022 Aug. Embryonic exposure to butylparaben and propylparaben induced developmental toxicity and triggered anxiety-like neurobehavioral response associated with oxidative stress and apoptosis in the head of zebrafish larvae. *Environ. Toxicol.* 37 (8), 1988–2004. <https://doi.org/10.1002/tox.23545>. Epub 2022 Apr 26. PMID: 35470536.
- Liu, C., Li, C., Hu, C., Wang, Y., Lin, J., Jiang, Y., Li, Q., Xu, X., 2018. CRISPR/Cas9-induced shank3b mutant zebrafish display autism-like behaviors. *Mol. Autism* 9, 23. <https://doi.org/10.1186/s13229-018-0204-x>.

- Liu, C., Wang, Y., Deng, J., Lin, J., Hu, C., Li, Q., Xu, X., 2021. Social deficits and repetitive behaviors are improved by early postnatal low-dose VPA intervention in a novel shank3-deficient zebrafish model. *Front. Neurosci.* 15.
- Livak, K.J., Schmittgen, T.D., 2001. Analysis of relative gene expression data using real-time quantitative PCR and the 2-(Delta Delta C(T)) method. *Methods* 25, 402–408. <https://doi.org/10.1006/meth.2001.1262>.
- Lucon-Xiccato, T., Dadda, M., 2017. Personality and cognition: sociability negatively predicts shoal size discrimination performance in guppies. *Front. Psychol.* 8.
- Lucon-Xiccato, T., Conti, F., Loosli, F., Foulkes, N.S., Bertolucci, C., 2020a. Development of open-field behaviour in the Medaka, *Oryzias latipes*. *Biology* 9, 389. <https://doi.org/10.3390/biology9110389>.
- Lucon-Xiccato, T., Di Mauro, G., Bisazza, A., Bertolucci, C., 2020b. Alarm cue-mediated response and learning in zebrafish larvae. *Behav. Brain Res.* 380, 112446. <https://doi.org/10.1016/j.bbr.2019.112446>.
- Lucon-Xiccato, T., Montalbano, G., Dadda, M., Bertolucci, C., 2020c. Lateralization correlates with individual differences in inhibitory control in zebrafish. *Biol. Lett.* 16, 20200296. <https://doi.org/10.1098/rsbl.2020.0296>.
- Ma, Y., Li, Y., Song, X., Yang, T., Wang, H., Liang, Y., Huang, L., Zeng, H., 2023 Feb 17. Endocrine disruption of Propylparaben in the male mosquitofish (*Gambusia affinis*): tissue injuries and abnormal gene expressions of hypothalamic-pituitary-gonadal-liver axis. *Int. J. Environ. Res. Public Health* 20 (4), 3557. <https://doi.org/10.3390/ijerph20043557>. PMID: 36834249; PMCID: PMC9967665.
- Matwiejczuk, N., Galicka, A., Brzoska, M.M., 2020. Review of the safety of application of cosmetic products containing parabens. *J. Appl. Toxicol.* 40, 176–210. <https://doi.org/10.1002/jat.3917>.
- McCarthy, D.J., Chen, Y., Smyth, G.K., 2012. Differential expression analysis of multifactor RNA-Seq experiments with respect to biological variation. *Nucleic Acids Res.* 40, 4288–4297. <https://doi.org/10.1093/nar/gks042>.
- Mei, Y., Monteiro, P., Zhou, Y., Kim, J.-A., Gao, X., Fu, Z., Feng, G., 2016. Adult restoration of Shank3 expression rescues selective autistic-like phenotypes. *Nature* 530, 481–484. <https://doi.org/10.1038/nature16971>.
- Merola, C., Lai, O., Conte, A., Crescenzo, G., Torelli, T., Alloro, M., Perugini, M., 2020a. Toxicological assessment and developmental abnormalities induced by butylparaben and ethylparaben exposure in zebrafish early-life stages. *Environ. Toxicol. Pharmacol.* 80, 103504. <https://doi.org/10.1016/j.etap.2020.103504>.
- Merola, C., Perugini, M., Conte, A., Angelozzi, G., Bozzelli, M., Amorena, M., 2020b. Embryotoxicity of methylparaben to zebrafish (*Danio rerio*) early-life stages. *Comp Biochem Physiol C Toxicol Pharmacol* 236, 108792. <https://doi.org/10.1016/j.cbpc.2020.108792>.
- Merola, C., Lucon-Xiccato, T., Bertolucci, C., Perugini, M., 2021. Behavioural effects of early-life exposure to parabens in zebrafish larvae. *J. Appl. Toxicol.* 41, 1852–1862. <https://doi.org/10.1002/jat.4171>.
- Meyer, M.P., Trimmer, J.S., Gilthorpe, J.D., Smith, S.J., 2005. Characterization of zebrafish PSD-95 gene family members. *J. Neurobiol.* 63, 91–105. <https://doi.org/10.1002/neu.20118>.
- Morbiato, E., Frigato, E., Dinarello, A., Maradonna, F., Facchinello, N., Argenton, F., Carnevali, O., Dalla Valle, L., Bertolucci, C., 2019. Feeding entrainment of the zebrafish circadian clock is regulated by the glucocorticoid receptor. *Cells* 8, 1342. <https://doi.org/10.3390/cells8111342>.
- Nishina, S., Kohsaka, S., Yamaguchi, Y., Handa, H., Kawakami, A., Fujisawa, H., Azuma, N., 1999. PAX6 expression in the developing human eye. *Br. J. Ophthalmol.* 83, 723–727. <https://doi.org/10.1136/bjo.83.6.723>.
- Nowak, K., Ratajczak-Wrona, W., Górska, M., Jabłońska, E., 2018. Parabens and their effects on the endocrine system. *Rev. Mol. Cell Endocrinol.* 15 (474), 238–251. <https://doi.org/10.1016/j.mce.2018.03.014>.
- Olley, G., Pradeepa, M.M., Grimes, G.R., Piquet, S., Polo, S.E., FitzPatrick, D.R., Bickmore, W.A., Boumendil, C., 2021. Cornelia de Lange syndrome-associated mutations cause a DNA damage signalling and repair defect. *Nat. Commun.* 12, 3127. <https://doi.org/10.1038/s41467-021-23500-6>.
- Orefice, L.L., Zimmerman, A.L., Chirila, A.M., Sleboda, S.J., Head, J.P., Ginty, D.D., 2016. Peripheral mechanosensory neuron dysfunction underlies tactile and behavioral deficits in mouse models of ASDs. *Cell* 166, 299–313. <https://doi.org/10.1016/j.cell.2016.05.033>.
- Peça, J., Feliciano, C., Ting, J.T., Wang, W., Wells, M.F., Venkatraman, T.N., Lascola, C. D., Fu, Z., Feng, G., 2011. Shank3 mutant mice display autistic-like behaviours and striatal dysfunction. *Nature* 472, 437–442. <https://doi.org/10.1038/nature09965>.
- Perez-Riverol, Y., Csordas, A., Bai, J., Bernal-Llinares, M., Hewapathirana, S., Kundu, D. J., Inuganti, A., Griss, J., Mayer, G., Eisenacher, M., Pérez, E., Uszkoreit, J., Pfeuffer, J., Sachsenberg, T., Yilmaz, S., Tiwary, S., Cox, J., Audain, E., Walzer, M., Jarnuczak, A.F., Ternent, T., Brazma, A., Vizcaíno, J.A., 2019. The PRIDE database and related tools and resources in 2019: improving support for quantification data. *Nucleic Acids Res.* 47, D442–D450. <https://doi.org/10.1093/nar/gky1106>.
- Perugini, M., Merola, C., Amorena, M., D'Angelo, M., Cimini, A., Benedetti, E., 2019. Sublethal exposure to propylparaben leads to lipid metabolism impairment in zebrafish early-life stages. *J. Appl. Toxicol.* 40, 493–503. <https://doi.org/10.1002/jat.3921>.
- Piñero, J., Saúch, J., Sanz, F., Furlong, L.I., 2021. The DisGeNET cytoscape app: Exploring and visualizing disease genomics data. *Comput. Struct. Biotechnol. J.* 19, 2960–2967. <https://doi.org/10.1016/j.csbj.2021.05.015>.
- R Core Team, 2021. R: a language and environment for statistical computing. R Foundation for Statistical Computing, Vienna, Austria. <https://www.R-project.org/>.
- Rastogi, S.C., Schouten, A., de Kruijf, N., Weijland, J.W., 1995. Contents of methyl-, ethyl-, propyl-, butyl- and benzylparaben in cosmetic products. *Contact Dermatit* 32, 28–30. <https://doi.org/10.1111/j.1600-0536.1995.tb00836.x>.
- Raudvere, U., Kolberg, L., Kuzmin, I., Arak, T., Adler, P., Peterson, H., Vilo, J., 2019. g: Profiler: a web server for functional enrichment analysis and conversions of gene lists (2019 update). *Nucleic Acids Res.* 47, W191–W198. <https://doi.org/10.1093/nar/gkz369>.
- Represa, A., Bur-Ari, Y., 2005. Trophic actions of GABA on neuronal development. *Trends in Neurosciences*, INMED/TINS special issue: multiple facets of GABAergic synapses, 28, 278–283. <https://doi.org/10.1016/j.tins.2005.03.010>.
- Risso, D., Ngai, J., Speed, T.P., Dudoit, S., 2014. Normalization of RNA-seq data using factor analysis of control genes or samples. *Nat. Biotechnol.* 32, 896–902. <https://doi.org/10.1038/nbt.2931>.
- Rodier, P.M., 1995. Developing brain as a target of toxicity. *Environ. Health Perspect.* 103 (Suppl. 6), 73–76. <https://doi.org/10.1289/ehp.95103673>.
- Sarowar, T., Grabrucker, A.M., 2016. Actin-dependent alterations of dendritic spine morphology in Shankopathies. *Neural Plast.* 2016, e8051861. <https://doi.org/10.1155/2016/8051861>.
- Schnörr, S.J., Steenbergen, P.J., Richardson, M.K., Champagne, D.L., 2012. Measuring thigmotaxis in larval zebrafish. *Behav. Brain Res.* 228, 367–374. <https://doi.org/10.1016/j.bbr.2011.12.016>.
- Shannon, P., Markiel, A., Ozier, O., Baliga, N.S., Wang, J.T., Ramage, D., Amin, N., Schwikowski, B., Ideker, T., 2003. Cytoscape: a software environment for integrated models of biomolecular interaction networks. *Genome Res.* 13, 2498–2504. <https://doi.org/10.1101/gr.1239303>.
- Sheng, M., Kim, E., 2000. The shank family of scaffold proteins. *J. Cell Sci.* 113 (Pt 11), 1851–1856. <https://doi.org/10.1242/jcs.113.11.1851>.
- Smith, K.W., Souter, I., Dimitriadis, I., Ehrlich, S., Williams, P.L., Calafat, A.M., Hauser, R., 2013. Urinary paraben concentrations and ovarian aging among women from a fertility center. *Environ Health Perspect.* Nov-Dec 121 (11–12), 1299–1305. <https://doi.org/10.1289/ehp.1205350>.
- Soni, M.G., Burdock, G.A., Taylor, S.L., Greenberg, N.A., 2001. Safety assessment of propyl paraben: a review of the published literature. *Food Chem. Toxicol.* 39, 513–532. [https://doi.org/10.1016/s0278-6915\(00\)00162-9](https://doi.org/10.1016/s0278-6915(00)00162-9).
- Soni, M.G., Carabin, I.G., Burdock, G.A., 2005. Safety assessment of esters of p-hydroxybenzoic acid (parabens). *Food Chem. Toxicol.* 43, 985–1015. <https://doi.org/10.1016/j.fct.2005.01.020>.
- Vandenberg, L.N., Bugos, J., 2021. Assessing the public health implications of the food preservative propylparaben: has this chemical been safely used for decades. *Curr. Environ. Health Rep.* 8, 54–70. <https://doi.org/10.1007/s40572-020-00300-6>.
- Večeřa, J., Bártová, E., Krejčí, J., Legartová, S., Komůrková, D., Rudá-Kučerová, J., Štark, T., Dražanová, E., Kaspárek, T., Šulcová, A., Dekker, F.J., Szymanski, W., Seiser, C., Weitzer, G., Mechoulam, R., Micale, V., Kozubek, S., 2018. HDAC1 and HDAC3 underlie dynamic H3K9 acetylation during embryonic neurogenesis and in schizophrenia-like animals. *J. Cell. Physiol.* 233, 530–548. <https://doi.org/10.1002/jcp.25914>.
- Vo, T.T.B., Yoo, Y.M., Choi, K.C., Jeung, E.B., 2010. Potential estrogenic effect(s) of parabens at the prepubertal stage of a postnatal female rat model. *Reprod. Toxicol.* 29 (3), 306–316.
- Wang, L.W., Tancredi, D.J., Thomas, D.W., 2011. The prevalence of gastrointestinal problems in children across the United States with autism spectrum disorders from families with multiple affected members. *J. Dev. Behav. Pediatr.* 32, 351–360. <https://doi.org/10.1097/DBP.0b013e31821bd06a>.
- Washbourne, P., 2015. Synapse assembly and neurodevelopmental disorders. *Neuropsychopharmacol* 40, 4–15. <https://doi.org/10.1038/npp.2014.163>.
- Wei, F., Mortimer, M., Cheng, H., Sang, N., Guo, L.-H., 2021. Parabens as chemicals of emerging concern in the environment and humans: a review. *Sci. Total Environ.* 778, 146150. <https://doi.org/10.1016/j.scitotenv.2021.146150>.
- Xu, B., Ionita-Laza, I., Roos, J.L., Boone, B., Woodrick, S., Sun, Y., Levy, S., Gogos, J.A., Karayiorgou, M., 2012. De novo gene mutations highlight patterns of genetic and neuronal complexity in schizophrenia. *Nat. Genet.* 44, 1365. <https://doi.org/10.1038/ng.2446>.
- Zarantonello, M., Randazzo, B., Gioacchini, G., Truzzi, C., Giorgini, E., Riolo, P., Gioia, G., Bertolucci, C., Osimani, A., Cardinaletti, G., Lucon-Xiccato, T., Milanović, V., Annibaldi, A., Tulli, F., Notarstefano, V., Ruschioni, S., Clementi, F., Olivetto, I., 2020. Zebrafish (*Danio rerio*) physiological and behavioural responses to insect-based diets: a multidisciplinary approach. *Sci. Rep.* 10, 10648. <https://doi.org/10.1038/s41598-020-67740-w>.
- Zhang, R., Wei, H., Xia, Y., Du, J., 2010. Development of light response and GABAergic excitation-to-inhibition switch in zebrafish retinal ganglion cells. *J. Physiol.* 588, 2557–2569. <https://doi.org/10.1113/jphysiol.2010.187088>.
- Zhang, X., Smits, A.H., van Tilburg, G.B., Ovaa, H., Huber, W., Vermeulen, M., 2018. Proteome-wide identification of ubiquitin interactions using UbIA-MS. *Nat. Protoc.* 13, 530–550. <https://doi.org/10.1038/nprot.2017.147>.